

## Versatile optical magnetoelectric effects by electromagnons in $\text{MnWO}_4$ with canted spin-spiral plane

Y. Takahashi,<sup>1,2,3</sup> S. Kibayashi,<sup>1</sup> Y. Kaneko,<sup>2</sup> and Y. Tokura<sup>1,2</sup>

<sup>1</sup>*Department of Applied Physics and Quantum Phase Electronics Center (QPEC), University of Tokyo, Tokyo 113-8656, Japan*

<sup>2</sup>*RIKEN Center for Emergent Matter Science (CEMS), Wako 351-0198, Japan*

<sup>3</sup>*PRESTO, Japan Science and Technology Agency, Chiyoda, Tokyo 102-8666, Japan*

(Received 30 August 2015; revised manuscript received 21 April 2016; published 13 May 2016)

The optical magnetoelectric (OME) effect based on electromagnon resonance has been investigated in a multiferroic helimagnet  $\text{MnWO}_4$  with the canted spin-spiral plane by the terahertz spectroscopy. Versatile OME effects emerge from the canted spin-spiral state, including the magnetochiral effect as manifested by the nonreciprocal directional dichroism. In addition to the transverse fluctuation mode of the spin-driven ferroelectric polarization, the electromagnon with a character of the longitudinal amplitude mode was found to cause the OME effect characteristic of the canted spin-spiral plane.

DOI: [10.1103/PhysRevB.93.180404](https://doi.org/10.1103/PhysRevB.93.180404)

Strong interactions between electricity and magnetism in matter, i.e., magnetoelectric (ME) effects, have been attracting increasing attention, because the cross-coupled responses to external stimuli lead to new functionalities of matter [1–4]. One such example is an optical phenomenon termed the optical magnetoelectric (OME) effect [5,6], for which both electric and magnetic dipole transitions are responsible. The OME effect is well exemplified by the nonreciprocal directional dichroism; the counterpropagating light beams in matter show different optical responses. Accordingly, different extinction coefficients,  $\kappa_+$  and  $\kappa_-$ , are observed for the light beams with propagation vectors  $+k^\omega$  and  $-k^\omega$ , respectively. Above all, the multiferroics, in which particular spin orders are responsible for ferroelectricity [7], exhibit strong OME effects on resonance of magnons endowed with electric dipole activity, i.e., electromagnons [8–13]. Since the OME effect is an ubiquitous phenomenon under the simultaneous breaking of time-reversal and space-inversion symmetries, the directional dichroism/birefringence have been reported recently for molecules [14–17], gas [18], metamolecules [19], and condensed matter [8–13,20–22], including artificial superlattices [23] in the frequency ranges of x-ray, visible, near infrared, terahertz, and gigahertz. However, a sizable OME effect compared to the parent resonance strength is still quite rare except for electromagnon resonances, even if the OME effect is allowed by symmetry. The OME effect always shows strong mode dependence, so that the mode character plays a crucial role. Accordingly, the clarification of characteristics of ME resonance is essentially important to elucidate the microscopic mechanism of the OME effect.

One of the most representative mechanisms of the multiferroics of spin origin is explained by the spin-current (SC) model [24] or the inverse Dzyaloshinskii-Moriya interaction [25,26], in which the microscopic polarization is described by cross product of neighboring spins;  $e_{ij} \times (S_i \times S_j)$ , where  $e_{ij}$  denotes the unit vector connecting neighboring spins ( $S_i$  and  $S_j$ ). This microscopic polarization turns out to be a ferroelectric polarization ( $P$ ) in a cycloidal spin structure [see Fig. 1(a)]. Accordingly, the spin waves or magnons in such a helimagnet inherently possess the fluctuation of  $P$ , i.e., the electric dipole moment, leading to the emergence of electromagnons [9,27,28].

In terms of the symmetry, the orthogonal  $P$  and magnetization ( $M$ ), which break both space-inversion and time-reversal symmetries, give rise to the OME effect for light with a propagation vector  $k^\omega \parallel P \times M$  [e.g., see Fig. 1(b)]; the sign of the directional dichroism is switched by the reversal of either  $P$  or  $M$  as shown in Fig. 1(c). The cycloidal spin structure, which spontaneously generates  $P$ , can induce the OME effect under the magnetic field normal to the cycloidal plane, because  $P \times M \neq 0$  [9,29]. In fact, the large OME effect has been observed on the resonance of the electromagnon in the cycloidal spin structure, in which the fluctuations of  $P$  and  $M$  are dynamically coupled with each other through the SC mechanism [9,12,29,30]. One other to the OME effect is given by the coexistence of  $M$  and chirality, which is specifically classified to the magnetochiral (MCh) effect, leading to the directional dichroism for the light propagating parallel to  $M$ ; the sign of the directional dichroism is switched by either the reversal of  $M$  or the change of the chirality [14,31]. Since the screw-spin structure [Fig. 1(a)], which has either clockwise or counterclockwise helicity, can provide the electronic chirality in matter irrespective of the symmetry of the chemical lattice, the MCh effect is allowed under the magnetic field [29,30]. For example the magnetic field normal to the spin plane induces the conelike screw spins with net magnetization, leading to the MCh effect [13,29,30]. In fact, the large MCh effect on the electromagnon resonance has been observed [13], in which the fluctuation of the conelike screw spins generates the transient cycloidal spin component, i.e., the dynamical polarization ( $\Delta P$ ), through the SC mechanism. Thus, the helimagnets inherently produce the OME effect on the electromagnon resonance.

In this Rapid Communication, we report the OME effect on the electromagnon resonance in a helimagnet  $\text{MnWO}_4$  by using terahertz spectroscopy. Since the canted spin-spiral plane in  $\text{MnWO}_4$  consists of the cycloidal and the screw spin components [see Fig. 1(a)], their spin dynamics provides an opportunity for comprehensive survey of the OME effects on the helical magnets. We observed the strong OME effects driven by the both cycloidal and screw-spin components on the electromagnon resonance. Furthermore, we found another OME resonance inherent to the canted spin-spiral plane, leading to the directional dichroism as large as 25% of

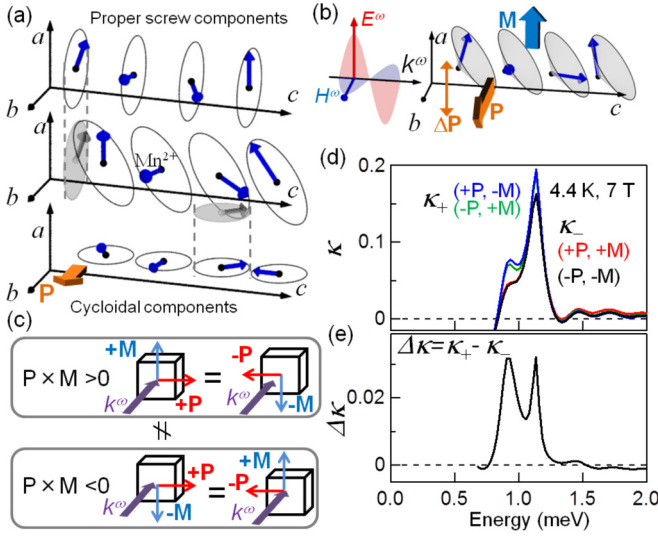


FIG. 1. (a) Schematics of the canted spin-spiral structure of  $\text{MnWO}_4$  (middle panel). The projections to the  $ab$  plane turn into a proper screw component (upper panel) and to the  $bc$  plane turn into the cycloidal spin components (lower panel). (b) The experimental geometry of light polarization ( $E^\omega \parallel a$ ,  $H^\omega \parallel b$ ), ferroelectric polarization ( $P \parallel b$ ), and induced magnetization ( $M \parallel a$ ) for the spin-spiral state in  $\text{MnWO}_4$ . (c) Classification of the states in terms of the optical magnetoelectric (OME) effect given by the signs of  $P$  and  $M$  (see text). (d) Extinction coefficient  $\kappa$  for the polarized light ( $E^\omega \parallel a$ ,  $H^\omega \parallel b$ ) at 4.4 K under the magnetic field (7 T). The signs of  $P$  and  $M$  for each spectrum are indicated. (e) Spectra of the OME effect ( $\Delta\kappa$ ) derived from the data in panel (d) (see text for definition).

parent electromagnon resonance. The amplitude mode of the ferroelectric polarization  $P$  was proven to play a crucial role for the dynamical ME coupling on the resonance.

A single crystal of  $\text{MnWO}_4$  was synthesized by the floating zone method, and the  $ab$ -plane and  $bc$ -plane samples with diameter of 3 mm were prepared. The time-domain terahertz spectroscopy was employed to measure the refractive indices by the experimental setup and procedures as detailed in Ref. [32]. The laser pulse with 100-fs duration from a Ti:sapphire laser was split into two paths to generate and detect the wave form of terahertz pulses. A bow-tie-shaped antenna and a dipole antenna were used for generation and detection of terahertz pulses, respectively. In order to manipulate the helicity of the spiral spins, the electric field ( $\sim 2$  kV/cm) was applied along the  $b$  axis while cooling the sample. The magnetic field was applied to the sample in Faraday ( $k^\omega \parallel H$ ) and Voigt ( $k^\omega \perp H$ ) geometries by using the superconducting magnets.

$\text{MnWO}_4$  has a monoclinic lattice structure with the monoclinic angle of  $\beta \sim 91^\circ$ . Below 12.7 K, the spin-spiral phase (AF2 phase), in which the spin-spiral plane cant from the  $a$  axis with an angle of  $35^\circ$ , takes place with a magnetic modulation vector  $q_m = (-0.214, 1/2, 0.457)$  [33] [see Fig. 1(a)]. As shown in Fig. 1(a), the projection of the canted spin spiral to the  $bc$  and the  $ab$  plane results in the cycloidal and the proper screw-spin components, respectively. Due to the cycloidal spin component, the ferroelectric polarization  $P \parallel b$  has been observed in the spin-spiral phase (AF2) [34,35], where the

helicity of the spin spiral is responsible for the sign of  $P$  in accord with the SC model [36].

Because the electromagnon ascribed to the transverse fluctuation of  $P$  is accessible by the light polarized perpendicular to  $P$ , i.e.,  $E^\omega \perp P$ , the light polarization with  $E^\omega \parallel a$  and  $H^\omega \parallel b$  is employed. An external magnetic field is applied along the  $a$  axis, so that the orthogonal  $P \parallel b$  and  $M \parallel a$  allows the OME effect for the light propagating along the  $c$  axis ( $\parallel k^\omega$ ) as shown in Fig. 1(b). Figure 1(d) shows the extinction coefficient  $\kappa$  under the magnetic field (7 T) at 4.4 K. Two distinct magnetic resonances are observed at 0.93 and 1.13 meV. The clear OME effect on these resonances is manifested by the directional dichroism, i.e., the difference of the peak magnitude under the reversal of either  $P$  or  $M$ . The spectral changes in line with the sign change of  $P \times M$  are consistent with the presence of the OME effect. The OME spectrum  $\Delta\kappa = \kappa_+ - \kappa_-$  can be defined by the difference between  $\kappa_+$  for  $P \times M > 0$  and  $\kappa_-$  for  $P \times M < 0$  [see Fig. 1(c)]. As shown in Fig. 1(e), the OME spectrum has two distinct peak structures; these magnetic excitations can be interpreted to be composed of both electric and magnetic dipole transitions, since both dipole activities are indispensable for the OME effect. Hence, they are assigned to the electromagnon.

To clarify the mode character of these resonances, their magnetic field and temperature dependencies were measured as shown in Figs. 2(c) and 2(d). At 4.5 K, the up-up-down-down collinear spin structure (AF1 phase) takes place below 2.6 T [see the phase diagram reproduced from [37] in

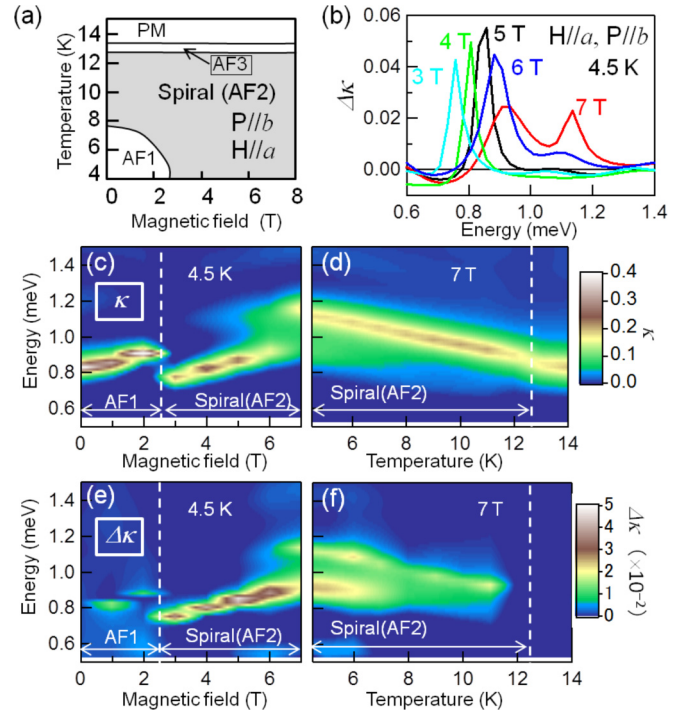


FIG. 2. (a) Magnetic phase diagram reproduced from Ref. [37] under a magnetic field along the  $a$  axis. (b) Magnetic field dependence of the OME spectra ( $\Delta\kappa$ ) for  $E^\omega \parallel a$ ,  $H^\omega \parallel b$  at 4.5 K. (c) The magnetic field dependence (4.5 K) and (d) the temperature dependence (7 T) of  $\kappa$ . (e) The magnetic field dependence (4.5 K) and (f) the temperature dependence (7 T) of the OME spectra ( $\Delta\kappa$ ).

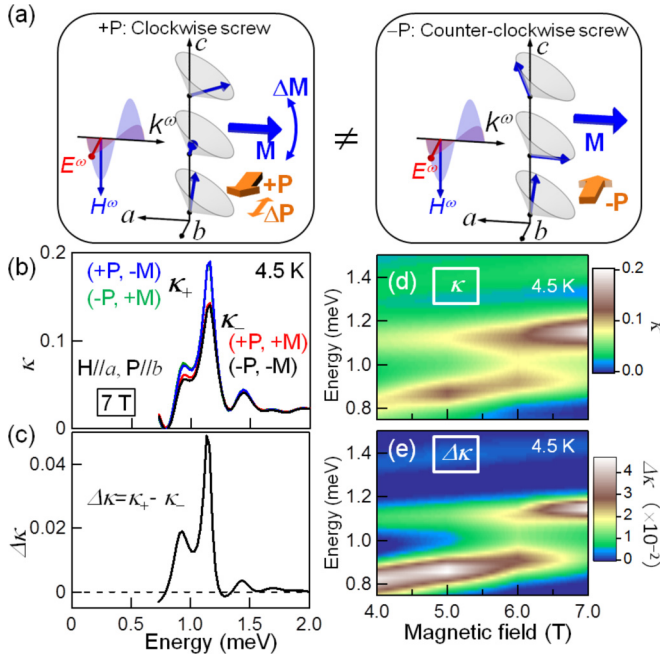


FIG. 3. (a) Schematics of the polarization of light ( $E^\omega \parallel b, H^\omega \parallel c$ ) and spin configurations. The helicities of spin orders with clockwise (left side) or counterclockwise (right side) are distinguished in term of the magnetochiral (MCh) effect (see text). (b) Spectra of  $\kappa$  for  $E^\omega \parallel b, H^\omega \parallel c$ . The signs of  $P$  and  $M$  for each spectra are indicated. (c) Spectrum of the OME effect ( $\Delta\kappa$ ) derived from panel (b). The magnetic field dependence of (d)  $\kappa$  and (e) the OME spectra ( $\Delta\kappa$ ) in the spin-spiral phase at 4.5 K.

Fig. 2(a)], showing an antiferromagnetic resonance (AFMR). The AFMR disappears upon the transition to the spin-spiral (AF2) phase at 2.6 T, while another mode of AFMR character for the spin-spiral phase shows up with the OME effect at slight lower energy [see Figs. 2(c) and 2(e)]. This lower-lying mode diminishes rapidly with increasing temperature due to the reduction of the spin-spiral order [see Figs. 2(d) and 2(f)]. These features are consistent with the results of inelastic neutron scattering studies [38,39]. With increasing magnetic field, the higher-lying mode can be seen above 5 T with the OME effect in addition to the lower-lying mode [see Figs. 2(c) and 2(e)]. This result suggests that the higher-lying mode arises from the fluctuation of the net magnetization. In fact, the higher-lying mode persists even in the higher temperature phases [see Figs. 2(d)], while the OME effect disappears [see Fig. 2(f)].

To survey the new ME resonance unique to the canted spin-spiral plane, we have investigated the OME effect in a different geometry, shown in Fig. 3(a). The magnetic field is applied along the  $a$  axis, so that the same spin orders as described in Fig. 1(b) take place, while the configuration of light polarization and propagation is different;  $E^\omega \parallel b, H^\omega \parallel c$  and  $k^\omega \parallel a$ , i.e.,  $E^\omega \parallel P$  and  $k^\omega \parallel M$ . In this geometry, the propagation vector of light ( $k^\omega$ ) is parallel to  $M$  and the proper screw component of the canted spin plane [see Fig. 1(a)] hosts the electronic chirality in matter, resulting in the OME effect as classified to the MCh effect. The helicity of the spin spiral is fixed by the sign of  $P$  arising from the cycloidal

components. Although the inevitable Faraday rotation affects the optical responses, the observed rotation angle is sufficiently small ( $< 20 \text{ mrad T}^{-1}$ ), allowing us to employ the quasilinear polarization analysis below 7 T. The magnetic resonances with two peaks are observed with clear directional dichroism as shown in Fig. 3(b). The reversal of  $P$ , which switches chirality, alters the optical responses, as well as the reversal of  $M$ , so that the presence of the MCh effect is clearly confirmed. The OME spectrum ( $\Delta\kappa$ ) in Fig. 3(c) shows two pronounced peaks, whose magnitude is as large as 25% of the parent electromagnon resonance. The magnitude of the OME spectra is comparable with the case of the former geometry in Fig. 1(e), while the development of the higher-lying mode is to be noted.

The SC model explains the OME effect on the electromagnons in the helimagnet including the cycloidal and the proper screw-spin structures [9,12,13,29,30]. For example, the rotatory oscillation of the cycloidal spin plane accompanies the transverse fluctuation of  $P$ , leading to the polarization selection rule of the electromagnon as  $E^\omega \perp P$  [9,27] as demonstrated in the configuration in Fig. 1(b). In contrast, the genuine cycloidal spin state cannot induce the longitudinal fluctuation mode of  $P$ , i.e., the stretching oscillation of  $P$ , resulting in the absence of the electromagnon for  $E^\omega \parallel P$ . Therefore the OME effect for  $E^\omega \parallel P$  observed here suggests a different character of the relevant electromagnon from those in the genuine cycloidal helimagnets. A possible mechanism stems from the canted spin-spiral plane in the  $\text{MnWO}_4$ . As shown in Fig. 3(a), the rotation of the spiral plane around the  $b$  axis accompanying  $\Delta M \parallel c$ , which is forced by the  $H^\omega \parallel c$ , produces a fluctuation of the cycloidal component in the  $bc$  plane, leading to the stretching or the amplitude oscillation of  $P$ . Accordingly the cross coupling between the  $\Delta P$  and  $\Delta M$  occurs on the electromagnon resonance. The observed OME effect under the reversal of  $M$  or of helicity of spins is consistently explained by this model. Thus the electromagnon for  $E^\omega \parallel P$  can be ascribed to the longitudinal amplitude mode of the ferroelectric polarization  $P$  endowed with the inherent ME coupling.

The appreciable enhancement of the OME effect by the intermode couplings between electromagnon and magnon or between electromagnon and electromagnon has been reported in the helimagnets [9,12]. As the magnetic field is increased, the increase of the OME effect for the higher-lying mode is observed, while the lower-lying mode decreases [see Fig. 3(e)] as is the case with the former setting in the Fig. 2(e). The intermode mixing between the observed two modes may be responsible for the appreciable magnitude of the directional dichroism for the lower-lying magnetic resonance in addition to the higher-lying mode of the genuine electromagnon character.

The screw-spin component [see Fig. 1(a)], which can generate the electronic chirality in matter, gives rise to the MCh effect in one other geometry [13,29,30]. Since the magnetic field along the  $c$  axis, which stabilizes the spin-spiral phase as shown in Fig. 4(b) [40], induces the canted conelike screw spin states [see Fig. 4(a)], the MCh effect is allowed with the light propagating along the  $c$  axis. In this geometry, the fluctuation of  $M$ , i.e., the inclination of cones, induces  $\Delta P$  through the SC model, so that the MCh effect for the light with  $k^\omega \parallel c$  is expected on the resonance of the electromagnon [29,30]. A

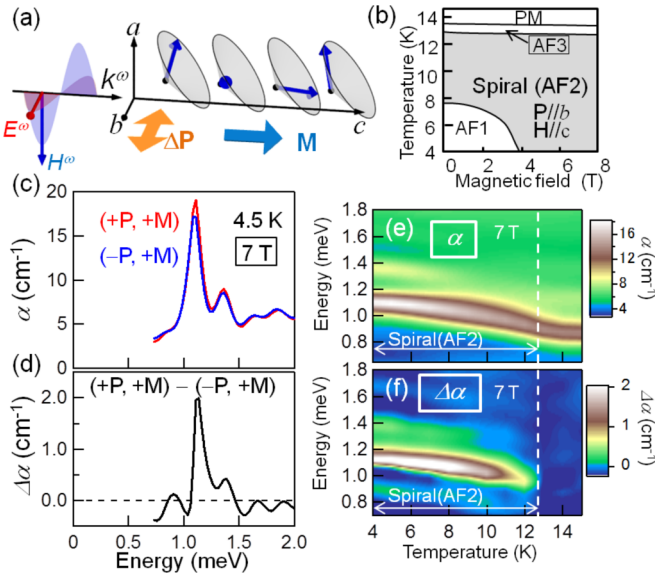


FIG. 4. (a) Schematics of geometry of the light polarization and the spin structure under the magnetic field along the  $c$  axis. (b) Magnetic phase diagram of  $\text{MnWO}_4$  reproduced from Ref. [40] under the magnetic field ( $H \parallel c$ ). (c) Absorption coefficient  $\alpha$  for the distinct states in terms of the OME effect at 7 T (see text). (d) Spectrum of the OME effect (directional absorption difference,  $\Delta\alpha$ ) derived from (c). The temperature dependence of (e)  $\alpha$  and (f) the OME spectra  $\Delta\alpha$  at 7 T.

sizable Faraday rotation prohibits the quasilinear polarization analysis in this case, so that we evaluate the absorption of light as described by the relation that  $\exp(-\alpha d) = (|E_{\parallel}^{sam}|^2 + |E_{\perp}^{sam}|^2) / (|E_{\parallel}^{ref}|^2 + |E_{\perp}^{ref}|^2)$ ; here  $E_{\parallel, \perp}^{ref, sam}$  are the orthogonal electric fields of light ( $\parallel$  and  $\perp$ ) through the sample ( $sam$ ) and the reference hole ( $ref$ ), respectively, and  $d$  is a sample

thickness. The reversal of the chirality is provided by the reversal of  $P$ . The difference of the absorption coefficient  $\alpha$  on the magnetic resonance [Figs. 4(c) and 4(d)] is observed under the change of chirality, equivalently the reversal of  $P$ , indicating the presence of the OME effect assigned to the MCh effect. The magnitude of the MCh effect ( $\Delta\alpha$ ) decreases with increasing temperature as shown in Fig. 4(f), while the resonance itself ( $\alpha$ ) still survives above the spin-spiral (AF2) phase [see Fig. 4(e)]. These results further confirm that the observed MCh effect on the electromagnon resonance originates from the spin-spiral structure.

In summary, we have investigated the OME effect of the electromagnons in  $\text{MnWO}_4$  with the canted spin-spiral plane. Both cycloidal and proper screw-spin components derived from the canted spin-spiral plane exhibit the OME effects observed as the directional dichroism. Furthermore, we found the electromagnon inherent to the canted spin-spiral plane, which is ascribed to the amplitude mode of the  $P$ , leading to the OME effect as classified to the MCh effect. The observed directional dichroism is as large as 25% of parent electromagnon resonance strength. Therefore, the both transverse fluctuation and longitudinal amplitude modes of the order parameter  $P$  of multiferroic helimagnets have been proven to cause electromagnon resonances hosting sizable OME effects. This mechanism for the OME effect can be applied to multiferroic soft magnets, such as hexaferrites, in which the canted spin spiral is easily formed under a modest magnetic field [41]. The electromagnon ascribed to the amplitude mode of  $P$  will be useful also for the coherent control of  $P$  through the recently developed high-field terahertz pulses [42].

This work was partly supported by the Japan Society for the Promotion of Science (JSPS) Grants-in-Aid for Scientific Research (No. 26706011 and No. 24224009) and the FIRST program by the Japan Society for the Promotion of Science (JSPS).

- [1] W. Eerenstein, N. D. Mathur, and J. F. Scott, *Nature (London)* **442**, 759 (2006).
- [2] J. F. Scott, *Science* **315**, 954 (2007).
- [3] Y. Tokura, S. Seki, and N. Nagaosa, *Rep. Prog. Phys.* **77**, 076501 (2014).
- [4] F. Matsukura, Y. Tokura, and H. Ohno, *Nat. Nanotech.* **10**, 209 (2015).
- [5] L. D. Barron, *Molecular Light Scattering and Optical Activity* (Cambridge University Press, Cambridge, UK, 2004).
- [6] T. Arima, *J. Phys. Condens. Matter* **20**, 434211 (2008).
- [7] T. Kimura, T. Goto, H. Shintani, K. Ishizaka, T. Arima, and Y. Tokura, *Nature (London)* **426**, 55 (2003).
- [8] I. Kézsmárki, N. Kida, H. Murakawa, S. Bordács, Y. Onose, and Y. Tokura, *Phys. Rev. Lett.* **106**, 057403 (2011).
- [9] Y. Takahashi, R. Shimano, Y. Kaneko, H. Murakawa, and Y. Tokura, *Nat. Phys.* **8**, 121 (2012).
- [10] S. Bordács, I. Kézsmárki, D. Szaller, L. Demkó, N. Kida, H. Murakawa, Y. Onose, R. Shimano, T. Rőöm, U. Nagel, S. Miyahara, N. Furukawa, and Y. Tokura, *Nat. Phys.* **8**, 734 (2012).
- [11] Y. Okamura, F. Kagawa, M. Mochizuki, M. Kubota, S. Seki, S. Ishiwata, M. Kawasaki, Y. Onose, and Y. Tokura, *Nat. Commun.* **4**, 2391 (2013).
- [12] Y. Takahashi, Y. Yamasaki, and Y. Tokura, *Phys. Rev. Lett.* **111**, 037204 (2013).
- [13] S. Kibayashi, Y. Takahashi, S. Seki, and Y. Tokura, *Nat. Commun.* **5**, 4583 (2014).
- [14] G. L. J. A. Rikken and E. Raupach, *Nature (London)* **390**, 493 (1997).
- [15] T. Roth and G. L. J. A. Rikken, *Phys. Rev. Lett.* **88**, 063001 (2002).
- [16] C. Train, R. Gheorghie, V. Krstic, L.-M. Chamoreau, N. S. Ovanesyan, G. L. J. A. Rikken, M. Gruselle, and M. Verdager, *Nat. Mater.* **7**, 729 (2008).
- [17] R. Sessoli, M.-E. Boulon, A. Caneschi, M. Mannini, L. Poggini, F. Wilhelm, and A. Rogalev, *Nat. Phys.* **11**, 69 (2014).
- [18] B. Pelle, H. Bitard, G. Bailly, and C. Robilliard, *Phys. Rev. Lett.* **106**, 193003 (2011).
- [19] S. Tomita, K. Sawada, A. Porokhnyuk, and T. Ueda, *Phys. Rev. Lett.* **113**, 235501 (2014).

- [20] G. L. J. A. Rikken, C. Strohm, and P. Wyder, *Phys. Rev. Lett.* **89**, 133005 (2002).
- [21] M. Saito, K. Ishikawa, and T. Arima, *J. Phys. Soc. Jpn* **77**, 013705 (2008).
- [22] M. Saito, K. Ishikawa, K. Taniguchi, and T. Arima, *Phys. Rev. Lett.* **101**, 117402 (2008).
- [23] N. Kida, H. Yamada, H. Sato, T. Arima, M. Kawasaki, H. Akoh, and Y. Tokura, *Phys. Rev. Lett.* **99**, 197404 (2007).
- [24] H. Katsura, N. Nagaosa, and A. V. Balatsky, *Phys. Rev. Lett.* **95**, 057205 (2005).
- [25] M. Mostovoy, *Phys. Rev. Lett.* **96**, 067601 (2006).
- [26] I. A. Sergienko and E. Dagotto, *Phys. Rev. B* **73**, 094434 (2006).
- [27] H. Katsura, A. V. Balatsky, and N. Nagaosa, *Phys. Rev. Lett.* **98**, 027203 (2007).
- [28] A. Pimenov, A. A. Mukhin, V. Yu. Ivanov, V. D. Travkin, A. M. Balbashov, and A. Loidl, *Nat. Phys.* **2**, 97 (2006).
- [29] S. Miyahara and N. Furukawa, *J. Phys. Soc. Jpn* **81**, 023712 (2012).
- [30] S. Miyahara and N. Furukawa, *Phys. Rev. B* **89**, 195145 (2014).
- [31] L. D. Barron and J. Vrbancich, *Mol. Phys.* **51**, 715 (1984).
- [32] N. Kida, Y. Ikebe, Y. Takahashi, J. P. He, Y. Kaneko, Y. Yamasaki, R. Shimano, T. Arima, N. Nagaosa, and Y. Tokura, *Phys. Rev. B* **78**, 104414 (2008).
- [33] G. Lautenschläger, H. Weitzel, T. Vogt, R. Hock, A. Böhm, M. Bonnet, and H. Fuess, *Phys. Rev. B* **48**, 6087 (1993).
- [34] K. Taniguchi, N. Abe, T. Takenobu, Y. Iwasa, and T. Arima, *Phys. Rev. Lett.* **97**, 097203 (2006).
- [35] A. H. Arkenbout, T. T. M. Palstra, T. Siegrist, and T. Kimura, *Phys. Rev. B* **74**, 184431 (2006).
- [36] H. Sagayama, K. Taniguchi, N. Abe, T. H. Arima, M. Soda, M. Matsuura, and K. Hirota, *Phys. Rev. B* **77**, 220407(R) (2008).
- [37] K. Taniguchi, N. Abe, S. Ohtani, and T. Arima, *Phys. Rev. Lett.* **102**, 147201 (2009).
- [38] H. Ehrenberg, H. Weitzel, H. Fuess, and B. Hennion, *J. Phys. Condens. Matter* **11**, 2649 (1999).
- [39] F. Ye, R. S. Fishman, J. A. Fernandez-Baca, A. A. Podlesnyak, G. Ehlers, H. A. Mook, Y. Wang, B. Lorenz, and C. W. Chu, *Phys. Rev. B* **83**, 140401(R) (2011).
- [40] K. Taniguchi, N. Abe, H. Sagayama, S. Otani, T. Takenobu, Y. Iwasa, and T. Arima, *Phys. Rev. B* **77**, 064408 (2008).
- [41] S. Ishiwata, Y. Taguchi, H. Murakawa, Y. Onose, and Y. Tokura, *Science* **319**, 1643 (2008).
- [42] T. Kampfrath, K. Tanaka, and K. A. Nelson, *Nat. Photon.* **7**, 680 (2013).